AIAA 82-4195

Low-Thrust Orbit Raising for Shuttle Payloads

T.M. Spencer*, R. Glickman,† and W. Bercaw‡
Ball Aerospace Systems Division, Boulder, Colo.

Most shuttle-launched satellites must ascend to higher orbits where air drag does not adversely affect lifetime and attitude control. A small hydrazine propulsion module can deliver the modest impulse typically required. Such low-energy transfers can be made using two extended low-thrust burns with negligible fuel penalty. In this paper, the propulsion module and the orbit transfer profile are optimized by minimizing the cost and complexity of onboard hardware and of ground support operations. The effects of thrust magnitude and of the ratio of final-to-initial orbit radius are studied numerically. The optimized orbit changing approach remains attractive for altitude changes up to about 7000 km. At that point, the hydrazine mass exceeds twice the payload mass, and the fuel penalty approaches 3% of the fuel required for a fuel-optimal Hohmann transfer.

Nomenclature

a	= semimajor axis
e	= eccentricity
p	= semilatus rectum $= a(1-e^2)$
r	= radius distance to center of attracting body
r_0, r_f	= initial, final circular radii
Δr	$= r_f - r_0$
R	= radial thrust acceleration
S	= azimuthal thrust acceleration
t	= time
ΔV_C	$= \Delta V$ for vanishingly small continuous thrust
ΔV_H	$= \Delta V$ for Hohmann transfer
ΔV_n	$= \Delta V$ for sum of n nested Hohmann transfers
X_1, X_2, X_3, X_4	= nonsingular orbit elements
θ	= true anomaly
μ	= gravitational constant
ρ	= radius ratio of final to initial orbits
ω	= argument of periapsis

Introduction

THE NASA Space Transportation System will not attain the desired operating altitude for most separable payloads. Typically, these free-flying spacecraft must ascend 100 to 600 km from one circular orbit to another. In many cases, it is desirable that they have the capability to descend at the end of their mission to make retrieval or refurbishment more convenient. For many, plane changes are also required.[1,2] Only altitude changes are treated here.

The impulse requirements for modest altitude changes are small compared to the capability of planned Spin-Stabilized Upper Stage (SSUS) and Inertial Upper Stage (IUS) vehicles.[3,4] This makes it attractive to consider smaller integrated monopropellant hydrazine orbit adjust systems. With such systems the total thrust time to achieve the required ΔV is typically greater than one orbit. While a classical, approximately impulsive Hohmann transfer is not possible, it is possible to visualize and implement the transfer as a series of many short burns. Such an "impulsive" profile is a natural extension of the state-of-the-art as applied to most past space missions.

In contast, there are significant advantages to using two extended burns. This low-thrust profile increases thruster reliability by avoiding many cold starts, reduces the total transfer time, reduces the cost of the initial intensive phase of ground support operations, and increases reliability by reducing the number of commands that must be properly conceived and executed.

Aside from the fact that a low-thrust transfer represents a change in standard practice, the potential disadvantages are that extended tracking intervals become desirable and that fuel penalties become a concern. The NASA Tracking and Data Relay Satellite System eliminates the first disadvantage. In fact, lower ascent rates offer the distinct advantages of increasing the time allowed for ground reaction in case of failures and increasing the allowances for burn application errors.

For altitude changes in the range of several hundred to several thousand kilometers, we find that fuel penalties are insignificant. For such transfers, optimal steering and throttling offer insignificant advantages and modest steering accuracy is acceptable. Thus, the potential fuel penalty is a myth. This myth exists partly because of the sheer bulk of published material on the optimization of low-thrust trajectories. Although our results on fuel efficiency represent relatively minor extensions of the work in a number of references, we have not found a sufficiently accurate treatment of low-thrust transfers between neighboring circular orbits.[5-7] We suspect that this is due partly to the lack of applications in the pre-shuttle era, partly to the fact that fuel optimization offers negligible benefits, and partly to the fact that accurate closed-form solutions are difficult over the variable ranges of interest.

For the range of thrust acceleration and altitude change we consider, the characteristics of the ascending and descending low-thrust trajectories change substantially. Lawden derived two approximate closed-form solutions; one for high and one for low thrust.[8] For low thrust, he observed that remarkable changes occur en route to escape, the solution indicating an early phase of transfers between nearby nearly circular orbits of increasing radius followed by a later phase of transfers between growing elliptical orbits. In fact, eccentricity never vanishes during a burn that starts from a precisely circular orbit.

To achieve the desired final circular orbit, it is necessary for the orbit eccentricity to vanish at the moment the desired semimajor axis is reached. We solve this problem by generating a "forward" low-thrust trajectory starting from the initial orbit, and a "backward" trajectory starting from the final orbit. Coast ellipses for patching from the first to the second trajectory are found by intersection of plots of eccentricity vs semimajor axis. For relatively large thrust, there is a unique patching orbit. There are many for low thrust and close orbits, roughly two for each revolution. While our approach appears to be a natural solution to this problem, we have found no reference describing it.

Presented at the 31st Congress of the International Astronautical Federation. Tokyo, Japan, Sept. 21-18, 1980; submitted Feb. 13, 1981; revision received Dec. 1, 1981.

*Chief Astrodynamicist. Member AIAA.
†Senior Space Systems Anaslyst. Member AIAA.
‡Applied Mathematician.

Our final result involves the optimization of a propulsion module to minimize the size, complexity, and the cost of the hardware and operational procedures required to accomplish orbit transfer. The resulting optimized low-energy propulsion module is slightly more complicated but more reliable and versatile than that used on the NASA Heat Capacity Mapping Mission (HCMM).[9] It is much less complicated and expensive than transfer vehicles and modules currently under development for shuttle payloads.[3,4,10]

Hardware Optimization

The details of optimization of the spacecraft hardware naturally depend on its payload and mission. Some aspects have broad applications, and these can be presented by treating a sample mission. We use the NASA Earth Radiation Budget Satellite (ERBS) for this purpose. This payload is small by shuttle standards, and it is important to minimize its length in the bay to minimize launch cost. The selected mechanical configuration is shown in Fig. 1.

The spacecraft bus is rectangular with a large volume available for payload instruments extending upward toward the bay doors. The instruments must be pointed at Earth during the ERBS mission. The propulsion module is in the lower structure that attaches the spacecraft to the orbiter keel. The ΔV thrusters point down in the figure. They must be pointed aft during orbit ascent. The planar arrangement of propellant tanks preserves the launch-cost-minimizing pancake shape. The ERBS weighs about 2000 kg.

The novel arrangement of four tightly clustered thrusters with their nozzles canted slightly outward provides reliable ΔV thrust, provides attitude control torques normal to the thrust axis, and minimizes the thrust disturbance torque about the thrust axis. This arrangement is attractive because it uses the minimum practical number of thrusters, because it minimizes plume impingement, and because it does not tightly constrain the spacecraft mass properties or the center of mass location.

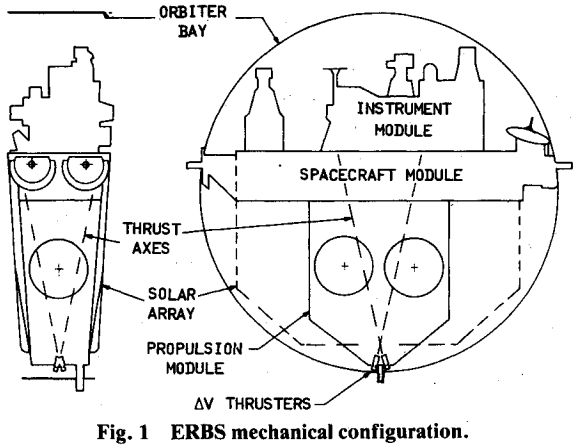

Fig. 1 ERBS mechanical configuration.

A single thruster, as used on HCMM is not practical because it would represent a single point failure for the critical orbit-raising function, and because the normal payload attitude control system cannot be expected to counteract typical thrust misalignment torques. Our thrusters are canted so that each has a large lever arm for attitude control torques. (We use 12 deg to provide 0.5 m control level arms, and we accept a small ΔV inefficiency of 2.2%). During burns, the potentially large transverse disturbance is controlled by periodically shutting down one of the four thrusters. Also, the thrusters can periodically fire during the normal mission to supplement or backup the normal attitude control system in two axes. Small thrusters and moderately large lever arms are typically required to efficiently produce backup attitude control torques. ERBS uses four additional thrusters (not shown) that enhance attitude control capability at the expense of added complexity and plume impingement problems.

While the lever arm for thrust components transverse to the ΔV axis is larger than 1 m, tight clustering of our thrusters keeps the lever arm for torques about the ΔV axis as small as 2 cm. If small enough thrusters are selected, this "pin-wheel" disturbance torque can be made comparable to the disturbances for which the normal payload control system is designed. For the ERBS mission we use 2 N thrusters. Typical 0.25 deg thrust misalignments correspond to a pin-wheel disturbance torque of only 0.0002 N-m.

The available normal attitude determination hardware depends on the payload mission. We assume that the system permits, or has been supplemented to permit, stabilization with respect to a rotating local vertical coordinate frame. ERBS is normally stabilized in that frame. It is only necessary to constrain the normal system hardware to permit attitude determination over the required altitude range and to require moderately high measurement bandwidths in transverse axes. Attitude errors of several degrees are acceptable.

Ascent Profile Optimization

It takes much less time and far fewer ground commands to follow a low-thrust instead of an impulsive profile. The latter would require nearly a hundred additional commands and roughly ten times the total transfer time used by the former. For small thrusters, total ascent time would be roughly one day compared to over a week. Larger thrusters would shorten ascent time, but they would increase the pin-wheel disturbance torque, they cannot deliver minimum torque impulses as small as typically desired for attitude control, they shorten allowed failure-correcting response time, and they increase chances of undesirable interaction with flexible structures.

Air drag disturbance torques are roughly one hundred times as large in the nominal 296 km shuttle orbit as in the final 600 km ERBS orbit. This makes it desirable to increase perigee altitude rather rapidly. To provide sufficient authority, the ΔV thrusters control attitude about axes normal to the velocity vector throughout the ascent phase. During burns, attitude is controlled simply by reducing the on-times of the

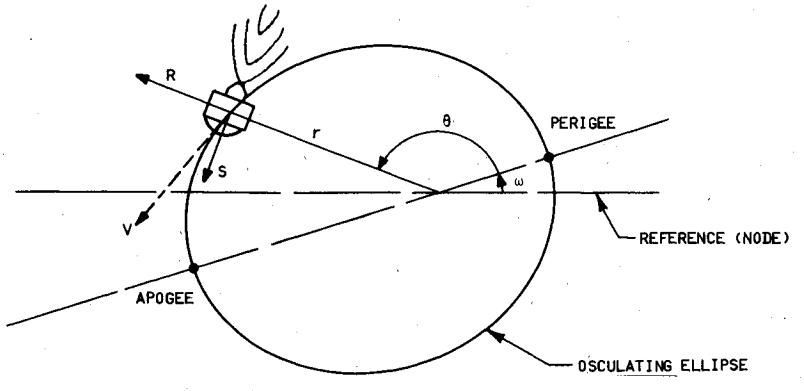

Fig. 2 Orbit geometry.

appropriate pair of thrusters. During coast, these thrusters do not waste fuel but they produce small unintentional ΔV's. For other thrusters both undesirable fuel waste and ΔV's can occur. The low-thrust profile minimizes these by minimizing coast time.

Orbit Transfer Geometry

Figure 2 depicts the osculating orbit at an instant during an ascent burn. (For clarity we will only treat orbit-raising missions henceforth). This orbit is a perturbation-free ellipse that is tangent to the perturbed trajectory at the satellite position. The orbit elements are instantaneous values of the time-varying perturbed elements. The rotating local vertical coordinate system is defined to align radial acceleration R with zenith and azimuthal acceleration S, normal to zenith in the direction and in the plane of orbital motion.

Figure 3 depicts the geometry for a typical low-thrust ascent between initial and final circular orbits. The transfer starts at the descending node, but this is arbitrary. The first extended burn raises the satellite from the initial circular orbit to a patch point on the elliptical coast orbit. This patching orbit is defined by the osculating orbit at first burn termination. It has the property that a hypothetical descent burn from an arbitrary point on the final circular orbit can reach an identical combination of semimajor axis and eccentricity.

The satellite must now coast in the patching orbit until it reaches an anomaly defined by the hypothetical descent trajectory. In order to reach the desired final semimajor axis and zero eccentricity simultaneously, the second burn must begin precisely at the second patch point. This point is the mirror image, about the major axis of the coast ellipse, of the point defined by the hypothetical descent burn.

Figure 3 depicts burn and coast arcs that are less than a complete revolution with respect to the reference line. Either burn can actually span a number of revolutions, and the satellite can make additional circuits of the coast ellipse. Our "optimized" ascent concept is best illustrated by transfers in which the first burn is a tight spiral spanning several revolutions.

Impulse-Approximating Transfers

Figure 4 is a two-dimensional schematic representation of "impulsive" transfers. Plots of eccentricity vs semimajor axis concisely represent crucial aspects of the transfers. Each point represents an orbit. Time history information is suppressed, and this greatly simplifies the representations.

The classical two-impulse Hohmann transfer is represented by the large triangle. The point at its apex defines the Hohmann transfer ellipse. An idealized perigee impulse would instantly move a and e from the left corner of the triangle (the initial circular orbit) to the apex. The apogee impulse moves a and e to the right corner (the final circular orbit). For high thrust, two short burns can quickly move a and e along the legs of the triangle, and can closely approximate the Hohmann.

For small thrust acceleration, there are two substantially different impulse-approximating profiles that accomplish the transfer. Profile A is represented by eight short burns that move a and e through short segments along the legs of the large triangle. The ends of each segment define intermediate coast orbits. For sufficiently short burns, the sum of the initial series of apogee-raising ΔV's (concentrated at perigee of the sequence of increasingly eccentric intermediate coast orbits) closely approximates the Hohmann perigee ΔV. The final sequence of perigee-raising apogee burns accumulate to approximate the Hohmann apogee ΔV. Disadvantages of profile A include the fact that perigee stays low through half the transfer, and that the total transfer time is long. Figure 5 shows that the satellite must coast through at least one complete orbit in each intermediate orbit.

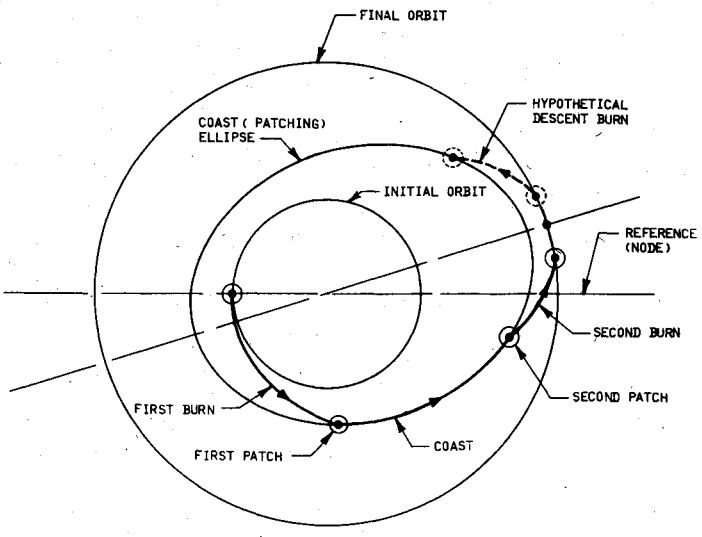

Fig. 3 Typical low-thrust ascent.

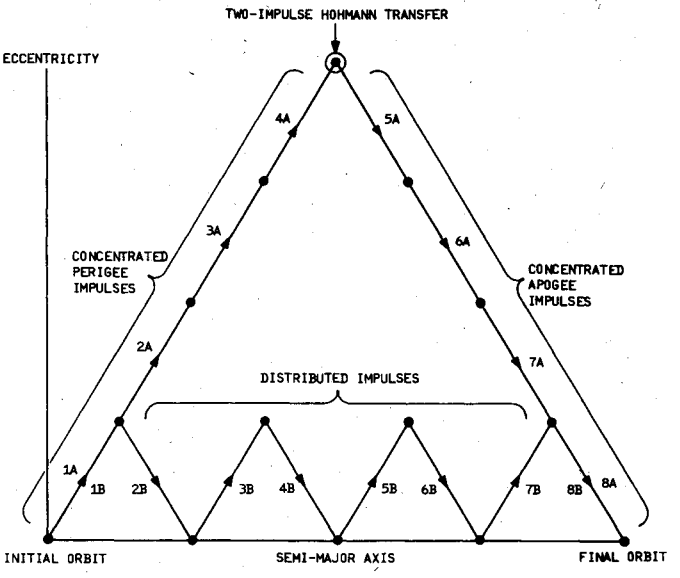

Fig. 4 Comparison of impulsive profiles.

Profile B provides a shorter total transfer time, raises perigee substantially sooner, and produces intermediate coast orbits of smaller eccentricity. It has the practical advantage that failure to complete the transfer would leave the payload in a more useful degraded orbit. As can be seen in Fig. 5, intermediate burns in profile B are distributed over a range of radii. The corresponding differences in preburn velocities compared to profile A cause energy losses, which lead to a fuel penalty for profile B.

We will show later that profile B can be closely approximated by continuous low thrust, and that neither suffers a significant fuel penalty for nearby orbits. For all impulsive profiles, we have ignored the small losses associated with finite burn time, and we have ignored the loss in thruster efficiency for short burns and cold starts.

Equations of Perturbed Orbital Motion

We use simplifying assumptions to make our comparison studies practical. We assume a spherical Earth, ignore all orbit perturbations other than thrust, and consider only planar transfers. While these simplifications exclude crucial details for real transfers, they do not significantly change the results of our comparison.

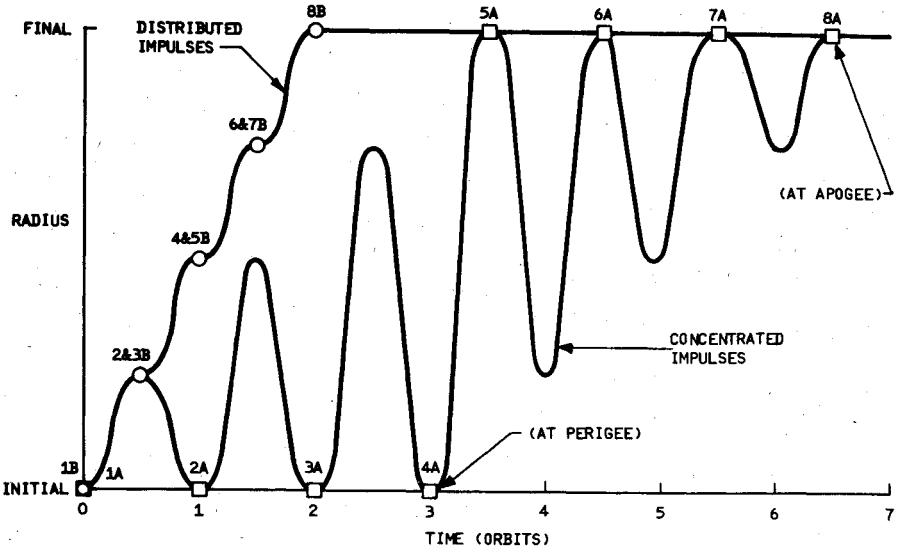

Fig. 5 Radius variation for impulsive profiles.

Because we are interested in burns that span many orbital revolutions, we use the variation of elements approach for special perturbations. Because orbit eccentricity initially vanishes and remains small, we use a nonsingular set of elements:

$$X_1 = a \qquad X_2 = e\sin\omega \qquad X_3 = e\cos\omega \qquad X_4 = \theta + \omega \quad (1)$$

Our perturbation equations are:

$$\frac{dX_1}{dt} = \frac{da}{dt}$$

$$\frac{dX_2}{dt} = \frac{de}{dt}\sin\omega + \left(e\frac{d\omega}{dt}\right)\cos\omega$$

$$\frac{dX_3}{dt} = \frac{de}{dt}\cos\omega - \left(e\frac{d\omega}{dt}\right)\sin\omega$$

$$\frac{dX_4}{dt} = \left(\frac{\mu}{p}\right)^{1/2}\left(\frac{1+e\cos\theta}{r}\right) \qquad (2)$$

where

$$\frac{da}{dt} = \frac{2a^2}{(\mu p)^{1/2}}\left[Re\sin\theta + S(1+e\cos\theta)\right]$$

$$\frac{de}{dt} = \left(\frac{p}{\mu}\right)^{1/2}\left[R\sin\theta + S\left(\cos\theta + \frac{e+\cos\theta}{1+e\cos\theta}\right)\right]$$

$$\frac{d\omega}{dt} = \frac{1}{e}\left(\frac{p}{\mu}\right)^{1/2}\left[-R\cos\theta + S\left(1+\frac{r}{p}\right)\sin\theta\right]$$

$$\frac{dE}{dt} = \left(\frac{\mu}{a}\right)^{1/2}\frac{1}{r} + \frac{1}{e\sin E}\left[\frac{de}{dt}\cos E - \frac{r}{a^2}\left(\frac{da}{dt}\right)\right] \qquad (3)$$

Equations (3) are classical Lagrange planetary equations as stated by Burt and Ehricke.[6,11] The singularity for $e=0$ in the next to last of Eq. (3) is avoided in the middle pair of Eq. (2), because $d\omega/dt$ only appears multipled by e. Our choice of X_4 allows us to eliminate the last of Eq. (3), and avoid a more serious singularity. This element is especially attractive because the last of Eq. (2) is not directly affected by the perturbation. A discussion by Townsend prompted us to use it.[12] Linearized perturbation equations are not accurate enough for our purposes.

Trajectories for Two Extended Burns

In this section, we present numerical data characterizing transfers between orbits as close together as 304 km (ERBS), and as far apart as 6674 km. The former gives $\Delta r = 0.046\, r_0$, and the later gives $\Delta r = r_0$. We compare thrust acceleration magnitudes large enough to approximate a Hohmann transfer and small enough to require nearly ten revolutions to complete the transfer. To simplify the interpretation of the data, we assume constant azimuthal thrust acceleration. Next, we treat two complications that must be considered for real missions; the effects of nonconstant thrust and error sensitivities. Finally, we summarize our fuel penalty data for low-thrust transfers.

For the 304-km ascent, Fig. 6 is a two-parameter representation of transfers for five thrust magnitudes. The solid paths describe the evolution of the osculating orbit, starting at the initial circular orbit in the lower left corner. The dashed paths are continuations of hypothetical descents, starting from the final circular orbit at the lower right corner.

For the highest thrust, the combined burn time is only 0.2 orbit, and the transfer closely approximates a Hohmann (see Fig. 4). The first and last burn each span about 0.1 orbit, and the total transfer time is just less than 0.5 orbit.

A factor of 5 lower thrust gives a total burn time of about one orbit. Three intersections occur; one shortly after first burn initiation, one after about 0.2 orbit, and one after nearly one orbit. The third intersection is preferred because it minimizes dispersions during the final burn. An additional 50% thrust reduction gives a two-orbit total burn time. Here, the three intersections are all near maximum eccentricity for this case. For the next lower thrust value, the burns span three revolutions, and there are seven intersections. For the lowest thrust, the burns span ten revolutions and give 21 intersections.

For sufficiently low thrust and small altitude changes, the paths can be approximated by cycloids. The semimajor axis increases at a nearly constant rate, so that eccentricity time histories have nearly identical shapes to those in Fig. 6. Eccentricity variations differ from precise cycloids in three respects that are important for accurate determination of the ascent trajectories. First, the peak eccentricity values are higher for descending than for ascending paths. Second, the period of cyclical variation is not constant. Third, there are secular growths of eccentricity, which are much smaller than the cyclical oscillations. This small effect is most easily seen for the two- and three-orbit burns. All three effects shift the intersections. The secular eccentricity trend has the crucial effect of preventing single burn transfers between precisely circular orbits.

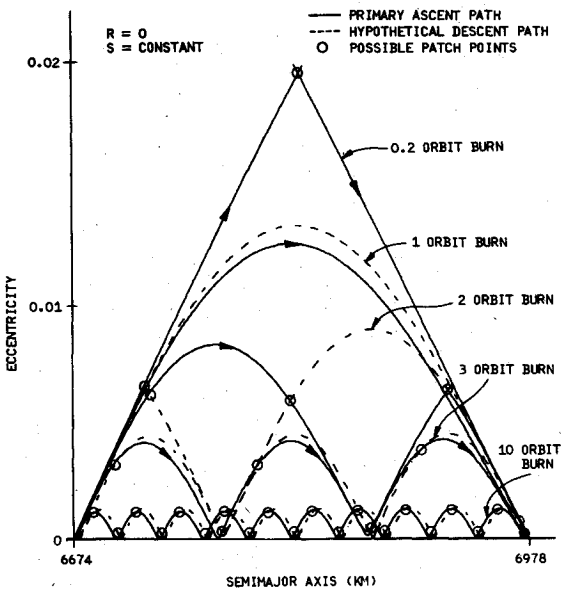

Fig. 6 Low-thrust transfers for $\Delta r = 0.046\, r_0$.

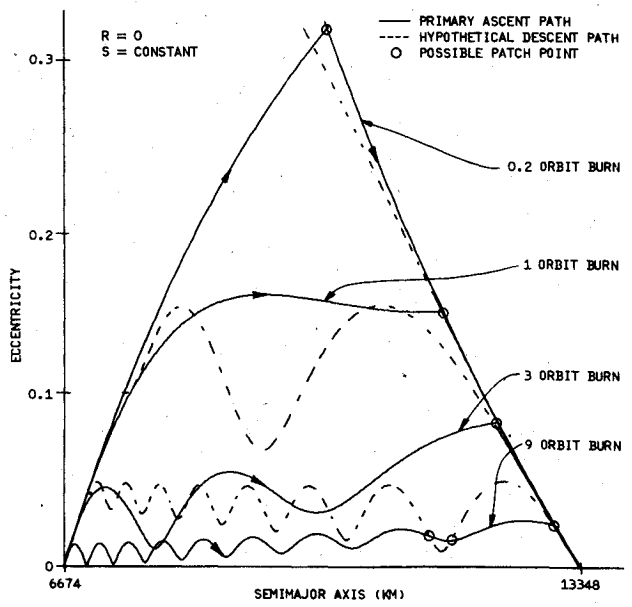

Fig. 8 Low-thrust transfer for $\Delta r = r_0$.

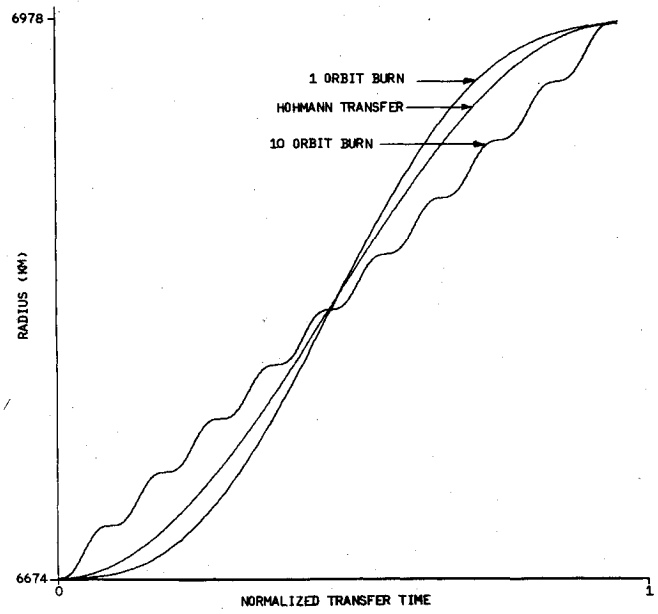

Fig. 7 Radius variation for $\Delta r = 0.046\, r_0$.

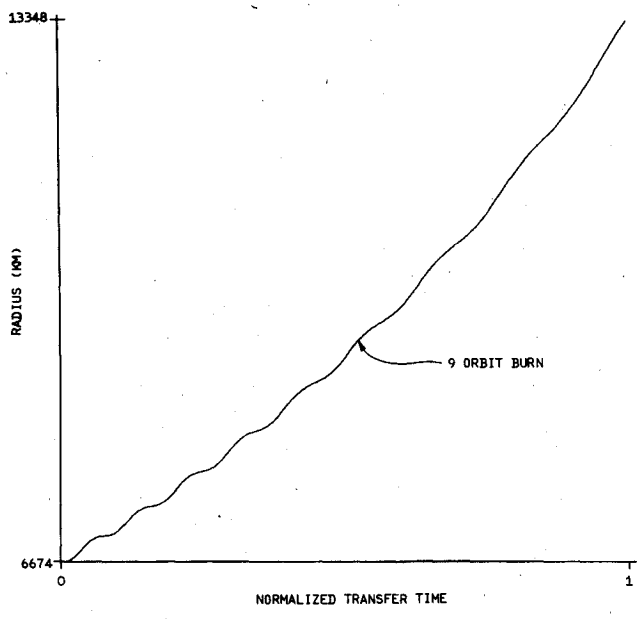

Fig. 9 Typical radius variation for $\Delta r = r_0$.

Figures 6 and 4 suggest that continuous low-thrust ascents are similar to those for a number of distributed impulses. This can be seen more clearly by comparing the radius time history for the ten-orbit burn in Fig. 7 with that on the left in Fig. 5. For a transfer this small, the continuous burn spanning one orbit provides ascent rates similar to those for a thrust-free Hohmann transfer (see Fig. 7.) For the smaller thrust levels, it is clear that continuous low-thrust ascents can be viewed as a set of transfers between nearly circular orbits of increasing radius.

Figures 8 and 9 show how transfer details change dramatically for larger transfer (e.g., $\Delta r = r_0$.) The sides of the triangle in Fig. 8, for the Hohmann-approximating largest thrust, are significantly bent. The size of the first cyclical peaks are substantially different for ascent and descent paths. The frequency of the cyclical variation decreases substantially during ascents, and increases substantially during descents. The secular trends are comparable to the cyclical variation. The amplitude of the cyclical variation decays with time in both cases. For the lower thrust levels depicted, there are fewer intersections than there were for smaller transfers.

It is clear from both Fig. 8 and the sample radius time history in Fig. 9 that the ascending trajectories only resemble transfers between nearby nearly circular orbits for early phases and for small thrust magnitude. These trajectories quickly pass into the later phase of sequential transfers between elliptical orbits of slowly increasing radius.

Thrust Variation and Error Sensitivity

For the small ERBS transfer, the characteristic velocity is only 170 m/s. This means the hydrazine mass used during ascent is less than 10% of the total mass. If fuel delivery pressure were regulated, thrust acceleration would be nearly constant. Unregulated "blowdown" systems are attractive because they are more reliable, and because they provide the lower thrust levels that are preferred later for on-orbit attitude control. This means thrust will decay by a factor of over two during the transfer.

Figure 10 shows how this decay affects the ascent and decent paths. Figure 10 should be compared with the ten-orbit burn in Fig. 6. (Note the different vertical scales.) The dashed

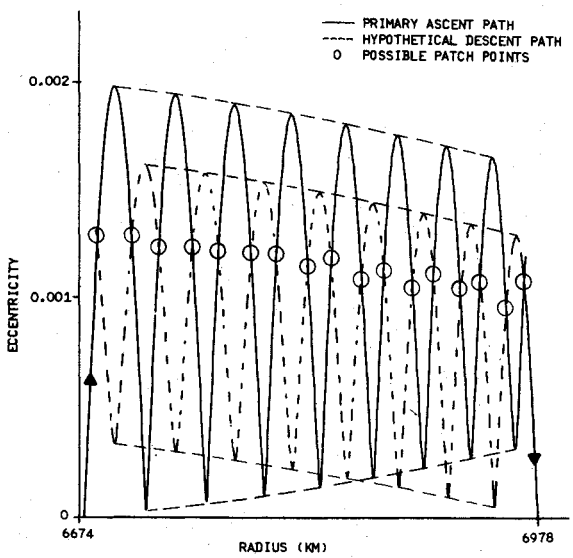

Fig. 10 ERBS transfer with variable thrust.

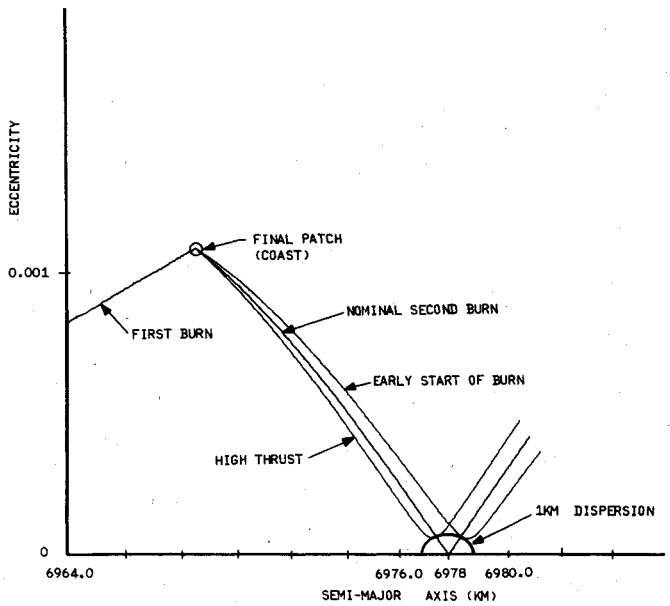

Fig. 11 ERBS error sensitivity.

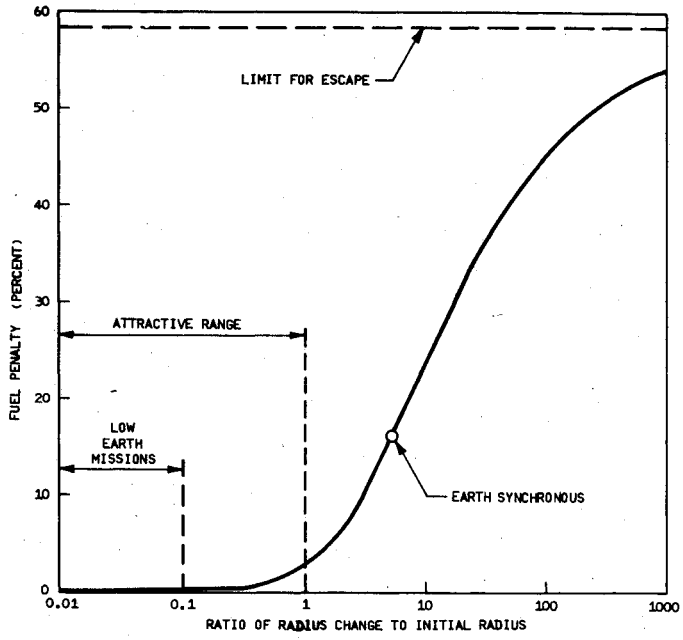

Fig. 12 Maximum penalty for low-thrust transfers.

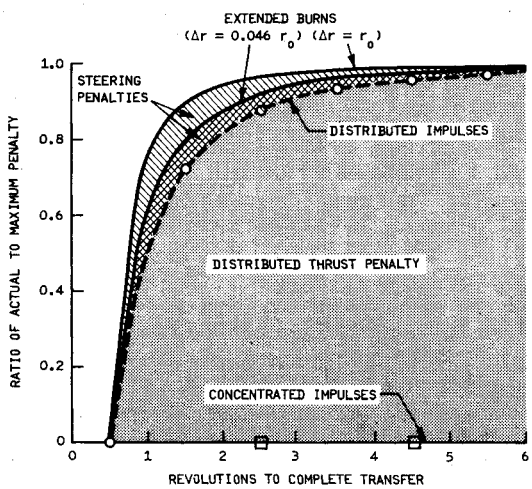

Fig. 13 Fuel penalty for extended and impulsive burns.

envelopes of extreme values of eccentricity show that decaying thrust produces substantial secular trends that were not present for constant thrust. For the ERBS case, we have 17 possible patch points and we choose the last one (farthest to the right).

Thrust errors prevent us from following the nominal trajectory. During the first long burn, our "guidance" technique is to compute new ascent and descent trajectories based on dispersions detected from tracking data. Dispersions slowly move the patch point, and may significantly change the first burn termination time. Small changes in the second burn termination time may adequately control the additional dispersion during the final burn.

For the ERBS case, Fig. 11 shows the small final dispersions caused by unexpectedly large errors of 10% in thrust magnitude, and 0.1 rad in coast angle (corresponding to a 100-s error in second burn initiation). Even for these pessimistic errors, the final paths are quite close to the desired one. Proper burn termination alone will constrain dispersions between the actual and desired final orbit to less than 1 km. (This corresponds to a 200-s allowance for burn termination on the nominal path.)

We have assumed a precisely circular initial orbit. However, our approach yields an efficient two-burn transfer so long as the initial eccentricity is sufficiently small (as determined by thrust magnitude and transfer size). Initial eccentricity can be at least as large as the peak value for the hypothetical descent. Near limiting values, it may be important to start the first burn on a particular segment of the initial orbit.

The classical Hohmann transfer between circular orbits requires[11]

$$\Delta V_H = \left(\frac{\mu}{r_0}\right)^{1/2}\left[\left(\frac{2\rho}{1+\rho}\right)^{1/2}\left(1-\frac{1}{\rho}\right)+\left(\frac{1}{\rho}\right)^{1/2}-1\right] \tag{4}$$

For vanishingly small constant azimuthal acceleration, the osculating ellipse of the densely wrapped ascent spiral achieves circularity once each revolution. The secular rate of radius increase[6] is

$$\frac{dr}{dt} = \frac{2r^{3/2}}{\mu^{1/2}} S \tag{5}$$

Integration yields the result also given by Arthur[13]:

$$\Delta V_c = \left(\frac{\mu}{r_0}\right)^{1/2}\left[1-\left(\frac{1}{\rho}\right)^{1/2}\right] = \left(\frac{\mu}{r_0}\right)^{1/2} - \left(\frac{\mu}{r_f}\right)^{1/2} \quad (6)$$

Thus, we have the surprising result that the required velocity increment is equal to the difference in circular velocities. For a range of changes in orbit altitude, Fig. 12 gives the low-thrust fuel penalty compared to a Hohmann transfer. The penalty is expressed as a percent of the fuel required for low thrust. Because it can be shown that Eq. (6) applies to both cases, the penalty is the same for small distributed impulses, and for continuous low thrust. It is clear that the penalty is virtually zero for typical near-Earth missions. It is about 3% for $\Delta r = r_0$.

This fuel penalty is called the "maximum" penalty for low thrust, because our trajectory integrations show that our fuel penalties increase monotonically with decreasing thrust, and that they accurately approach our theoretical value for vanishing thrust. These data are summarized in Fig. 13. Thrust gets smaller toward the right, while the vertical scale gives the penalty numerically determined for a specific thrust and transfer size. The penalty is expressed as a fraction of the value plotted in Fig. 12. We see that actual penalties never exceeded that "maximum" value.

In Fig. 13, we also plot our theoretical result for distributed impulses:

$$\Delta V_n = \left(\frac{\mu}{r_0}\right)^{1/2}(1-\rho^{-1/2})\left[\left(\frac{2}{1+\rho^{-1/n}}\right)^{1/2}(1+\rho^{-1/2n})-1\right] \quad (7)$$

(When $n = 1$, Eq. (7) gives the classical Hohmann result.)

Our results for extended burns always show slightly higher penalties, after carefully defining transfer revolutions in each case. (Impulsive transfers can be properly represented only by discrete points.) For distributed impulses; the difference in penalty for $\Delta r = 0.046\, r_0$ and $\Delta r = r_0$ is too small to plot.

We characterize the major portion of the fuel penalty in Fig. 13 as the energy loss caused by distributing the thrust over a range of radii. The remainder is a steering loss. These penalties only become significant for large transfers such as to Earth synchronous orbit. In that case, more efficient steering should be considered.

Conclusions

Two extended low-thrust burns can efficiently transfer many shuttle payloads to nearby higher circular orbits. The fuel penalty is negligible compared to the more conventional approach of using many short burns. The low-thrust approach is faster, less expensive, and more reliable than the conventional approach. A small integrated hydrazine propulsion module is sufficient for many missions. The module can be configured to avoid added shuttle launch costs. As few as four thrusters can reliably provide the required ΔV and can back up normal attitude control in two axes.

References

[1] Spencer, T.M., Glickman, R., and Porcelli, G., "Changing Inclination for Shuttle Payloads," *Journal of Guidance and Control,* Vol. 2, July-Aug. 1979, pp. 264-270.

[2] Lang, T.J., "Optimal Impulsive Maneuvers to Accomplish Small Plane Changes in an Elliptical Orbit," *Journal of Guidance and Control,* Vol. 2, July-Aug. 1979, pp. 271-275.

[3] "Special Report: Space Shuttle, Transportation System of the Future," *Aviation Week and Space Technology,* Vol. 105, Nov. 8, 1976, pp. 36-154.

[4] "Spinning Solid Upper Stage for Delta and Atlas/Centaur Class Missions," (Study 2.6) Final Report, Aerospace Corporation, Los Angles, Calif., Aerospace Report ATR-76 (7377-01)-01, Vols. I and II.

[5] Edelbaum, T.N., "Optimum Low-Thrust Transfer Between Circular and Elliptic Orbits," *Proceedings of the Fourth U.S. National Congress on Applied Mechanics,* American Society of Mechanical Engineers, New York, 1962, pp. 137-141.

[6] Burt, E.G.C., "On Space Maneuvers with Continuous Thrust," *Planetary Space Sciences,* Vol. 15, Pergamon Press Ltd., Northern Ireland, 1967, pp. 103-122.

[7] Gobetz, F.W., "A Linear Theory of Optimum Low-Thrust Rendezvous Trajectories," *Journal of the Astronautical Sciences,* Vol. XII, Fall 1965, pp. 69-70.

[8] Lawden, D.F., "Optimal Escape from a Circular Orbit," *Astronautica Acta,* Vol. 4, June 1958, pp. 218-223.

[9] "Heat Capacity Mapping Mission (HCMM) Launch," NASA TM-79429, April 1978.

[10] Myers, S. and Raymond, H., "MMS—A Systems Level View of Standardization," Paper AAS 79-026, Rocky Mountain Guidance and Control Conference, Keystone, Colo., Feb. 1979.

[11] Ehricke, K.A., *Space Flight,* Vols. I and II, Van Nostrand Co., Inc., New York, 1962.

[12] "Orbital Flight Handbook," NASA SP33, 1963.

[13] Arthur, P.D., "Low Thrust Orbit Penalty," *ARS Journal,* Sept. 1961, pp. 1273-1275.